

Fast and Effective Robustness Certification for Recurrent Neural Networks

Wonryong Ryou¹ Jiayu Chen¹ Mislav Balunović¹ Gagandeep Singh¹ Andrei Dan² Martin Vechev¹

Abstract

We present a precise and scalable verifier for recurrent neural networks, called R2. The verifier is based on two key ideas: (i) a method to compute tight linear convex relaxations of a recurrent update function via sampling and optimization, and (ii) a technique to optimize convex combinations of multiple bounds for each neuron instead of a single bound as previously done. Using R2, we present the first study of certifying a non-trivial use case of recurrent neural networks, namely speech classification. This required us to also develop custom convex relaxations for the general operations that make up speech preprocessing. Our evaluation across a number of recurrent architectures in computer vision and speech domains shows that these networks are out of reach for existing methods as these are an order of magnitude slower than R2, while R2 successfully verified robustness in many cases.

1. Introduction

Prior work demonstrated susceptibility of recurrent neural networks (RNNs) to adversarial perturbations of its inputs (Papernot et al., 2016). Naturally, this exposed serious security vulnerabilities in state-of-the-art speech recognition models based on RNNs (Carlini & Wagner, 2018; Li et al., 2019). As recurrent networks are widely used in other tasks which require modeling long-term dependencies, such as the games of Dota (Pachocki et al., 2018) and StarCraft (Vinyals et al., 2019), verifying robustness of recurrent architectures has become an important challenge towards deployment of these models in practice.

In this work, we consider the problem of certifying robustness of recurrent neural networks. We illustrate the problem setting and overall flow in Fig. 1. Here, the labeled rectangles represent the operations in the network we are certifying. We focus on LSTMs as the most widely used form

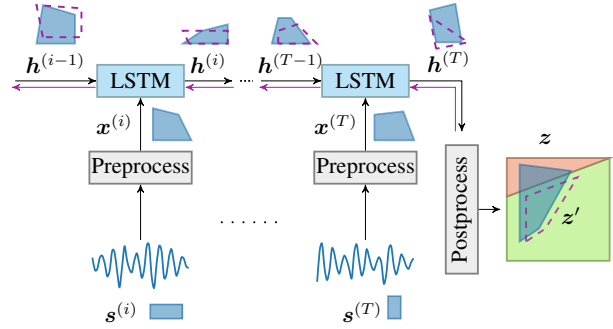


Figure 1. End-to-end certification of RNNs using R2: we show how all possible perturbations are captured and propagated through the system, then refined backward for better precision.

of RNNs, but the method can be easily extended to other architectures such as GRUs. The “Preprocess” boxes capture domain-specific pre-processing operations (typically present when using RNNs, e.g., speech processing). At each timestep i , pre-processing receives a convex shape $s^{(i)}$, which captures all possible inputs obtained by adding perturbations to the original input. Certification of LSTMs is then based on propagating these convex shapes through both the preprocessing operations and the LSTM network itself, and results in a convex shape in the output, denoted as z . If z contains only output vectors which classify to the correct class, robustness of the LSTM network is established.

Key challenge: convex relaxations for LSTMs The key challenge to effective certification of LSTMs is the design of convex relaxations of non-convex operations: given a convex shape capturing the hidden state $h^{(i-1)}$, to produce the shape capturing the next state $h^{(i)}$. A recent method (Ko et al., 2019) computes this relaxation by using gradient-based optimization, but suffers from two major issues. First, the optimization procedure is expensive and does not scale to realistic use cases. Second, even if we disregard scalability, the method lacks convergence and optimality guarantees. To address these issues, we introduce a novel technique based on a combination of sampling and linear programming, which is significantly more precise and scalable than Ko et al. (2019), while also offering asymptotic guarantees of convergence towards the optimal

¹Department of Computer Science, ETH Zürich, Zürich, Switzerland ²ABB Corporate Research, Baden-Dättwil, Switzerland.

solution.

Refinement via optimization As mentioned earlier, to certify the property, we need to verify if each concrete point in the output shape z classifies to the correct label. If this is true, then we have proved the output of the network is correct on all inputs in the input convex regions $s^{(1)}, \dots, s^{(T)}$. However, as in Fig. 1, when we propagate these shapes through the network, due to over-approximation, it is possible to obtain an output shape z which contains spurious incorrect concrete points (it intersects the red region representing incorrect outputs). To address this issue, we form a loss based on the output shape, backpropagate the gradient of this loss through the timesteps and adjust the convex relaxations in each LSTM unit to decrease the loss so that in the next try we arrive closer to certifying the network. This is demonstrated in Fig. 1 using the purple backward arrows with the new convex shapes shown in purple. Finally, the new output shape z' (dashed purple) lies completely inside the green region of the output space, meaning it contains only (provably) correct output vectors and hence certification succeeds. As we show experimentally, this method significantly increases precision of end-to-end certification, without introducing large runtime costs. We remark that advances in certification introduced in our work are also of interest beyond RNNs, especially the method to dynamically choose between different convex relaxations.

Key contributions Our main contributions are:

- A novel and efficient method to certify robustness of recurrent neural networks to adversarial perturbations. The method is based on new convex relaxations which handle non-linear operations in LSTMs, significantly more scalable and precise than prior work.
- A novel method which dynamically selects between multiple convex relaxations in order to increase certification precision.
- An implementation of the method in a system called R2. We evaluated R2 on several benchmarks and datasets, showing it scales to realistic networks. Further, using R2, we were able to, for the first time, certify RNNs used in speech classification.

Related work While the first adversarial examples for neural networks were found in computer vision (Szegedy et al., 2013; Biggio et al., 2013), recent work also showed the vulnerability of RNNs (Papernot et al., 2016). Modern speech recognition systems, based on RNNs, were shown susceptible to small noise crafted by an adversary using white-box attacks (Carlini et al., 2016; Carlini & Wagner, 2018), achieving 100% success rate against DeepSpeech (Hannun et al., 2014). These were

later followed by inaudible attacks (Qin et al., 2019), universal perturbation (Neekhara et al., 2019), structural analysis (Yang et al., 2019), and adversarial music (Li et al., 2019). While providing a good empirical estimate of the vulnerability of RNNs, these works do not provide any robustness guarantees, which is the goal of our work.

Much recent work also aims at certifying neural networks, typically using SMT solving (Katz et al., 2017), abstract interpretation (Gehr et al., 2018; Singh et al., 2018), Lipschitz optimization (Ruan et al., 2018), linear relaxations (Zhang et al., 2018; Weng et al., 2018; Salman et al., 2019; Singh et al., 2019a), symbolic intervals (Wang et al., 2018b), semi-definite relaxations (Raghunathan et al., 2018b) or combinations of methods (Wang et al., 2018a; Singh et al., 2019c). Another line of work considers using these relaxations to train provably robust neural networks (Wong & Kolter, 2017; Raghunathan et al., 2018a; Mirman et al., 2018; Goyal et al., 2018; Zhang et al., 2020; Balunovic & Vechev, 2020). However, they do not train provably robust recurrent networks: to achieve this, our convex relaxations could be combined with these training methods.

There has also been recent work on certification of RNNs. Akintunde et al. (2019) propose certification of RNNs based on mixed-integer linear programming, but it can only be applied to ReLU networks and does not work for LSTMs, which have sigmoid and tanh activations. Wu & Kwiatkowska (2019) propose a discretization method to certify video models that are a combination of CNNs and RNNs. However, discretization does not scale to the perturbations we consider in our work. Esmailpour et al. (2019) address the certification of support vector machines for audio classification, but do not support neural networks. The most related work to ours is POPQORN (Ko et al., 2019), which proposes a method to certify RNNs. However, their approach is based on expensive gradient-based optimization, which does not scale to practical applications such as audio classification, as we show in our experiments. Lyu et al. (2019) propose to adjust the linear relaxations of activation functions, such as ReLU, tanh, and sigmoid by using projected gradient descent. Their approach shares the idea of learning the linear relaxation, but is restricted to feed-forward networks, and does not consider the more challenging case of learning the convex combination of bounds for non-linearities in LSTMs. Recent work also certifies Transformers (Shi et al., 2020) using linear relaxations of non-linear operations in that architecture. However, they do not consider using multiple linear relaxations as we do. Jacoby et al. (2020) propose to verify RNNs by automatically inferring the temporal homogeneous invariants using binary search. However, their approach is limited to vanilla RNNs and does not apply to more commonly used LSTM networks which

we consider in this work.

2. Overview

In this section we use a small illustrative example to introduce our certification method. Our goal is to certify robustness of a single LSTM cell with respect to the input $x \in [-1.2, 1.2]$. In this example, for the sake of simplicity, we assume there are two output classes and all intermediate LSTM gates $\{\mathbf{i}, \mathbf{f}, \mathbf{g}, \mathbf{o}\}$ share weight matrices and biases:

$$\begin{aligned} \{\mathbf{i}, \mathbf{f}, \mathbf{g}, \mathbf{o}\} &= \begin{bmatrix} 1 \\ 0.5 \end{bmatrix} x + \begin{bmatrix} 0 \\ 1 \end{bmatrix} \\ \mathbf{c} &= \sigma(\mathbf{i}) \odot \tanh(\mathbf{g}) \\ \mathbf{h} &= \sigma(\mathbf{o}) \odot \tanh(\mathbf{c}). \end{aligned}$$

To certify robustness, we need to prove that $h_2 - h_1 > 0$, implying the neural network classifies the input to label 2.

Interval bound propagation (IBP) The simplest approach is based on propagating concrete interval bounds through the LSTM operations, disregarding the relationships between variables. Using this method to certify the network in our example, we obtain:

$$\begin{aligned} c_1 &\in [-0.64, 0.64] & h_1 &\in [-0.43, 0.43] \\ c_2 &\in [0.23, 0.77] & h_2 &\in [0.13, 0.54]. \end{aligned}$$

Using the above values results in the lower bound $h_2 - h_1 \geq -0.30$. Clearly, this inequality does not allow us to prove $h_2 - h_1 > 0$, and results in the failure of certification.

Linear relaxation via linear program The main issue with interval bounds is that they do not track relationships between variables in the sequence of operations. To address this, we compute lower and upper linear relaxations of each non-linear operation in the neural network.

We demonstrate our approach for calculating a lower linear relaxation of $h_2 = \sigma(o_2) \tanh(c_2)$. The input domain is $o_2 \in [0.4, 1.6]$ (note that $o_2 = 0.5x + 1$ here) and $c_2 \in [-0.79, 0.62]$. First, we uniformly sample the set of points $\{(x_1, y_1), \dots, (x_n, y_n)\}$ from the input domain $[0.4, 1.6] \times [-0.79, 0.62]$. Then, we solve the following optimization problem to calculate the lower linear relaxation of h_2 :

$$\min_{A_l, B_l, C_l \in \mathbb{R}} \sum_{i=1}^n (\sigma(x_i) \tanh(y_i) - (A_l x_i + B_l y_i + C_l)),$$

subject to the constraint that $A_l x_i + B_l y_i + C_l \leq \sigma(x_i) \tanh(y_i)$ for each i . This is a linear program that can be solved efficiently in polynomial time. However, the obtained bound may not be sound as the sampled points do not fully cover the continuous input domain. To address this, we shift the plane downwards by an offset (decreasing C_l)

equal to the maximum violation between $A_l x + B_l y + C_l$ and h_2 . After solving the linear program and the adjustment, we obtain $A_l = 0.02, B_l = 0.48, C_l = 0.00$ which results in the following lower linear relaxation to h_2 : $h_2 \geq LB_{h_2} = 0.02o_2 + 0.48c_2 + 0.00$. We compute the upper bound analogously.

Note that prior work (Ko et al., 2019) uses more expensive gradient-based optimization to obtain coefficients A_l, B_l, C_l which is orders of magnitude slower than our efficient method based on linear programming.

After computing a linear relaxation of each neuron, we calculate via back-substitution, the lower bound of $h_2 - h_1$

$$\begin{aligned} &\geq (0.02o_2 + 0.48c_2 + 0.00) - (0.12o_1 + 0.22c_1 + 0.15) \\ &\geq 0.02o_2 + 0.48(0.18i_2 + 0.38g_2 - 0.12) \\ &\quad - 0.12o_1 - 0.22(0.18i_1 + 0.17g_1 + 0.23) - 0.15 \\ &\geq 0.29(0.5x + 1) - 0.20x - 0.25 \\ &\geq -0.06x + 0.04 \geq -0.03. \end{aligned}$$

While we obtain more precise bounds than intervals, this linear relaxation is not enough to certify robustness.

Optimization through multiple relaxations While our method based on linear programming offers efficient ways to compute linear relaxations of key functions, its main limitation is that it is static: if certification fails, there is no way to revisit the bounds and try again. In this work, we introduce a method which, upon failure of certification, makes a backward pass and adjusts the bounds to increase precision of the certification. Here, we calculate 4 additional planes for each bound, which we refer to as *candidate bounds*. We split the original input region $[l_x, u_x] \times [l_y, u_y]$ along two diagonals into 4 triangular regions which we denote as T_k , $k \in \{1, 2, 3, 4\}$. We also set T_0 equal to the full region. For each T_k we now perform the same sampling and optimization procedure as before:

$$\begin{aligned} &\min_{A_l, B_l, C_l \in \mathbb{R}} \sum_{i=1}^n (\sigma(x_i) \tanh(y_i) - (A_l x_i + B_l y_i + C_l)) \\ &\text{subject to } \bigwedge_{i=1}^n A_l x_i + B_l y_i + C_l \leq \sigma(x_i) \tanh(y_i) \\ &\text{where } (x_i, y_i) \sim T^k \end{aligned}$$

Finally, for each T_k , we obtain the following five candidate linear relaxations:

$$\begin{aligned} h_1 &\geq LB_{h_1}^0 = 0.12o_1 + 0.69c_1 - 0.16 \\ h_1 &\geq LB_{h_1}^1 = -0.16o_1 + 0.21c_1 - 0.20 \\ h_1 &\geq LB_{h_1}^2 = -0.04o_1 + 0.21c_1 - 0.08 \\ h_1 &\geq LB_{h_1}^3 = -0.16o_1 + 0.21c_1 - 0.20 \\ h_1 &\geq LB_{h_1}^4 = 0.19o_1 + 0.60c_1 - 0.27 \end{aligned}$$

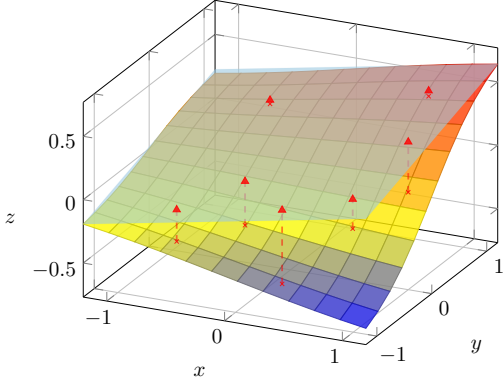


Figure 2. Visualization of the $z = \sigma(x) \tanh(y)$ curve and the upper bound computed by linear programming. Red crosses represent the sampled points and dashed arrows show the difference between the curve and the plane (summands in the optimization).

Note that $LB_{h_1}^0$ denotes the linear relaxation calculated from the whole region. The resulting lower bound LB_{h_1} is

$$LB_{h_1} = \sum_{k=0}^4 \lambda_k \cdot LB_{h_1}^k, \quad \sum_{k=0}^4 \lambda_k = 1.$$

Our optimization algorithm, explained later in Section 3.2, produces $\lambda = (0.34, 0.08, 0.16, 0.25, 0.18)$. Using this approach, we can prove that $h_2 - h_1 \geq 0.02 > 0$, enabling us to certify robustness of the LSTM network.

Compared to Ko et al. (2019), which commit to a single bound, our method is more flexible and can tune λ parameters to find a combination of 5 different bounds for each neuron that yields the most precise certification result.

3. Scalable Certification of LSTMs

In this section, we give technical details of our method for certification of LSTM networks. We first explain how to obtain tight linear bounds on key operations in the LSTM unit: $\sigma(x) \tanh(y)$ and $\sigma(x)y$. Then, we present a novel method to dynamically choose between different convex relaxations in order to increase the precision of the certifier.

3.1. Computing linear relaxation of LSTM operations

Here, our goal is to bound the product of sigmoid and tanh, using lower and upper bound planes parameterized by coefficients A_l, B_l, C_l and A_u, B_u, C_u , respectively:

$$A_l x + B_l y + C_l \leq \sigma(x) \tanh(y) \leq A_u x + B_u y + C_u$$

We formulate the search for a lower bound of $\sigma(x) \tanh(y)$ as an optimization problem with the aim to minimize the volume between the bound and the function, subject to the

constraint that the lower bound is below the function value:

$$\begin{aligned} \min_{A_l, B_l, C_l} \int_{(x,y) \in B} (\sigma(x) \tanh(y) - (A_l x + B_l y + C_l)) \\ \text{subject to } A_l x + B_l y + C_l \leq \sigma(x) \tanh(y), \forall (x, y) \in B. \end{aligned} \quad (1)$$

Here, we denote $B = [l_x, u_x] \times [l_y, u_y]$ as the boundaries of input neurons x and y . Prior work (Ko et al., 2019) solves this optimization problem using gradient-based methods which is both expensive and lacks convergence guarantees. Instead, we propose to solve Eq. (1) via sampling and linear programming, which is significantly faster and more precise than prior work, as we demonstrate experimentally.

Step 1: Approximation via LP In the first step, we solve an approximation of an intractable optimization problem from Eq. (1), obtaining potentially unsound constraints. We build on the approach from Balunovic et al. (2019) which proposes to approximate the objective in Eq. (1) using Monte Carlo sampling. Let $D = \{(x_1, y_1), \dots, (x_n, y_n)\}$ be a set of points from B sampled uniformly at random. We phrase the following optimization problem:

$$\begin{aligned} \min_{A_l, B_l, C_l \in \mathbb{R}} \sum_{i=1}^n (\sigma(x_i) \tanh(y_i) - (A_l x_i + B_l y_i + C_l)) \\ \text{subject to } \bigwedge_{i=1}^n A_l x_i + B_l y_i + C_l \leq \sigma(x_i) \tanh(y_i). \end{aligned} \quad (2)$$

In Fig. 2 we show an input region with Monte Carlo samples as red circles and summands in the LP objective as vertical lines. As this is a linear program (LP), we can solve it exactly in polynomial time using off-the-shelf LP solvers. We compute an upper bound analogously.

Step 2: Adjusting the offset to guarantee soundness

Due to the LP approximation, the resulting lower bound from the previous step may contain the point where the lower bound has a higher value than the true function, making it unsound. Balunovic et al. (2019) address this by computing the maximum soundness violation and adjusting the lower bound plane downwards to guarantee soundness. However, they use expensive branch-and-bound technique which do not scale to our setting. Instead, we show that in the case of the function $\sigma(x) \tanh(y)$, we can compute the maximum violation using a closed-form solution in constant time. More formally, let $\Delta_l = \max_{(x,y) \in B} \sigma(x) \tanh(y) - (A_l x + B_l y + C_l)$ be obtained using our closed-form formula. Then, we adjust the lower bound downwards by updating the offset $C_l \leftarrow C_l - \Delta_l$, resulting in a sound lower bound plane. We also update the upper bound analogously. Fig. 2 shows the upper bound

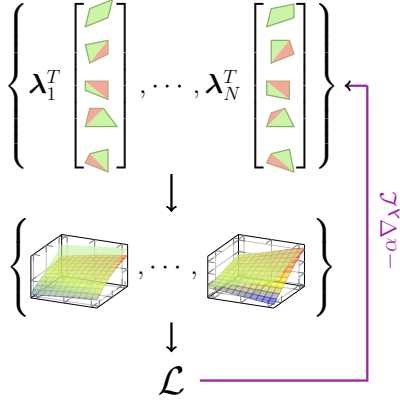


Figure 3. Learning to combine linear bounds via gradient descent. Here the 5 candidate planes multiplied by λ are depicted either in green or red, or both. Green represents the sampled domain, T_k , and red is the extension of the obtained green plane out of the domain. With the linear combination of the planes, we compute the bound, calculate the loss, and backpropagate.

plane obtained after solving the LP and adjusting the offset. Finally, we can prove that, similarly to Balunovic et al. (2019), as we increase the number of samples n , the solution of the LP asymptotically approaches the solution of the original problem from Eq. (1). We provide more details in Appendix.

3.2. Optimizing the combination of bounds

While our approach is based on sampling, linear programming and offset adjustment allow us to obtain an (asymptotically) optimal lower bound plane, it still has a fundamental limitation that it produces a *single* lower bound plane. Although the lower bound plane from Section 3.1 is optimal in terms of volume, this approach is, in a sense, greedy: when considering the *entire* network, it is possible that we can select non-optimal planes for each neuron, which yield more precise result in the end. Neither the method from Ko et al. (2019) nor our method from Section 3.1 can achieve this – we now present the first approach which can learn how to select bounds for the entire network so as to increase end-to-end precision of the certification.

Step 1: Compute a set of candidate bounds In the first step, we adapt our approach from Section 3.1 to produce a diverse set of candidate planes instead of a single plane. At a high level, we are going to run our Monte Carlo sampling procedure several times, each time on a different subdomain of the original domain $B = [l_x, u_x] \times [l_y, u_y]$ (however the constraints are still enforced over the entire domain). We define 4 different triangular subdomains: T_1 and T_2 are triangles resulting from splitting B along the main diagonal, while T_3 and T_4 are triangles resulting from split-

ting B along the other diagonal. We additionally define $T_0 = B$.

Now, for each $k \in \{0, 1, 2, 3, 4\}$, we perform sampling and optimization as in Eq. (2), this time sampling from T_k :

$$\begin{aligned} \min_{A_l, B_l, C_l \in \mathbb{R}} \sum_{i=1}^n (\sigma(x_i) \tanh(y_i) - (A_l x_i + B_l y_i + C_l)) \\ \text{subject to } \bigwedge_{i=1}^n A_l x_i + B_l y_i + C_l \leq \sigma(x_i) \tanh(y_i) \\ \text{where } (x_i, y_i) \sim T_k \end{aligned}$$

Additionally, for each k we also enforce the constraints at the corners of B . For each neuron i , this yields 5 candidate lower bound and upper bound planes, LB_i^k and UB_i^k for $k \in \{0, 1, 2, 3, 4\}$. These 5 candidate planes for each of the N neurons are shown in Fig. 3.

Step 2: Find the optimal combinations of the bounds

After computing a set of candidate bounds, in the next step our goal is to learn a convex combination of these bounds which yields the highest end-to-end certification precision. To do this, we define lower and upper bound of neuron i as a convex combination of the proposed 5 bounds:

$$\begin{aligned} LB_i &= \sum_{k=0}^4 \lambda_i^{LB} \cdot LB_i^k, \quad \sum_{k=0}^4 \lambda_i^{LB} = 1, \\ UB_i &= \sum_{k=0}^4 \lambda_i^{UB} \cdot UB_i^k, \quad \sum_{k=0}^4 \lambda_i^{UB} = 1. \end{aligned}$$

Recall that we formulate robustness certification as proving that for all labels i different from the ground truth label t :

$$z_t - z_i > 0$$

Here, the lower bound on $z_t - z_i$ is computed using back-substitution (Singh et al., 2019b), as shown in our overview example in Section 2. However, this lower bound now depends on the coefficients λ , so we define function $f(x, \epsilon, i, \tilde{\lambda})$ which computes the lower bound of the expression $z_t - z_i$ when using λ to combine the neuron bounds.

We describe our approach to find the best coefficients λ in Algorithm 1. In order to find λ , we solve the following optimization problem for each label i :

$$z_t - z_i \geq \max_{\lambda} f(x, \epsilon, i, \lambda)$$

If the solution to the above optimization problem is positive, then we have established robustness with respect to the class i . First, we initialize unnormalized $\tilde{\lambda}$ for each neuron uniformly between -1 and 1. Then, in each epoch we compute the normalized λ by applying softmax to $\tilde{\lambda}$ and

Algorithm 1 Learning λ via gradient descent

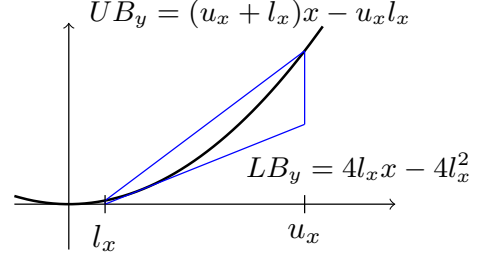
Given input x , label y , model \mathcal{M} , perturbation ϵ
for $i \leftarrow 1$ **to** m **where** $i \neq y$ **do**
 Initialize $\tilde{\lambda} \sim [-1, 1]^{N_{\text{bounds}} \times 5}$.
 $epoch \leftarrow 0$
repeat
 $\lambda \leftarrow \text{SoftMax}(\tilde{\lambda})$
 $\tilde{\mathcal{L}} \leftarrow -f(x, \epsilon, i, \lambda)$
 $\tilde{\lambda} \leftarrow \tilde{\lambda} - \alpha \nabla_{\tilde{\lambda}} \tilde{\mathcal{L}}$
 $epoch \leftarrow epoch + 1$
until $epoch = \text{max_epoch}$ or $\mathcal{L} \geq 0$
if $\mathcal{L} \geq 0$ **then**
 return not certified
end if
end for
return certified

then run the certification using λ , obtaining loss \mathcal{L} equal to the value $-f(x, \epsilon, i, \lambda)$. We then perform gradient descent update on $\tilde{\lambda}$ based on the loss. If at some point the loss is negative, it means we have just found λ which enables us to prove robustness and the algorithm terminates. The core updating flow is also shown visually in Fig. 3.

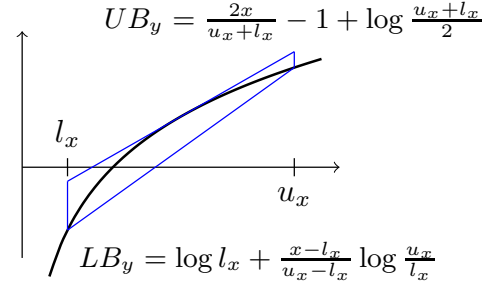
Note that, although we use gradient-based methods in certification as (Ko et al., 2019), the ideas are fundamentally different: in terms of runtime, we apply the optimization for each label which is typically at most 10 times per input, while they optimize for each $\sigma(x) \tanh(y)$ operation which too expensive for networks consisting of thousands of neurons. Further, we use optimization to adjust the bounds, while they use it to obtain a single bound, which produces even worse results than our method from Section 3.1.

4. Certification of Speech Preprocessing

We demonstrate the scalability of R2 by certifying, for the first time, the robustness of a speech classifier using LSTMs. Though there have been various works which operate directly on the raw signal (Pascual et al., 2017; Sainath et al., 2015), the *filterbank method*, or *log Mel-filterbank energy*, is most widely used speech preprocessing. The key challenge in the speech domain is to design linear convex relaxations for the non-linear operations in the preprocessing. The idea of filterbank is to model non-linear human acoustic perception as power spectrum filters based on certain frequencies, called *Mel-frequencies*. The final result of the transformation is a vector of coefficients whose elements contain log-scaled values of filtered spectra, one for every Mel-frequency. Sahidullah & Saha (2012) presented an approach to represent most computations, such as pre-emphasizing and FFT, using matrix multiplications. Below we discuss the main steps for handling



(a) Linear relaxation for square function.



(b) Linear relaxation for log function.

Figure 4. Two relaxations for the speech preprocessing stage.

non-linear preprocessing operations.

Square To handle L_2 norm computation, we provide linear relaxation of the square function, shown in Fig. 4a. We calculate the lower and upper linear bounds of $y = x^2$, where $x \in [l_x, u_x]$, as:

$$LB_y = \begin{cases} 4l_x x - 4l_x^2 & 0 \leq l_x < u_x/3 \\ 4u_x x - 4u_x^2 & 0 \geq 3u_x > l_x \\ 0 & l_x \leq 0 \leq u_x \\ (u_x + l_x)x - ((u_x + l_x)/2)^2 & o.w. \end{cases}$$

$$UB_y = (u_x + l_x)x - u_x l_x.$$

Log To handle computation of the logarithm of the power spectrum, we provide linear relaxation of the log function, shown in Fig. 4b. We calculate the lower and upper linear bounds of $y = \log x$, where $x \in [l_x, u_x]$, as:

$$LB_y = \log l_x + \frac{x - l_x}{u_x - l_x} \log \frac{u_x}{l_x}$$

$$UB_y = \frac{2x}{u_x + l_x} - 1 + \log \frac{u_x + l_x}{2}.$$

5. Experimental Evaluation

We now evaluate the effectiveness of R2 for certifying LSTM networks.

Setup We implemented R2 in PyTorch (Paszke et al., 2017) and used Gurobi 9.0 to solve linear programs. Com-

comparisons with POPQORN and scalability tests are performed on a single Nvidia GeForce GTX 1080 GPU. We use single Nvidia GeForce RTX 2080 GPU for the remaining experiments. Following convention from prior work (Singh et al., 2019b), we consider only those inputs that were correctly classified without perturbation. We use the same set of hyperparameters for all experiments. We use 100 sampling points in the linear program and optimize λ parameters using Adam (Kingma & Ba, 2014) for 200 epochs. During optimization, we initialize the learning rate to 100 and multiply it by 0.98 after every epoch.

5.1. Image classification

We first evaluate R2 on the image classification task proposed by Ko et al. (2019). They use the MNIST dataset (LeCun et al., 2010) and flatten each image into a vector of dimension 784. Then, this vector is partitioned into a sequence of k frames (k depends on the experiment). This frame sequence is then used as an input to the LSTM.

Comparison with POPQORN We now compare precision and scalability of R2 with POPQORN (Ko et al., 2019). We closely follow the evaluation setup used in the experiments of Ko et al. (2019). We trained an LSTM network containing 1 layer with 32 hidden units using standard training and achieved accuracy of 94.8%. The network receives a sequence of $k = 7$ image slices as input and predicts a digit corresponding to the image. We evaluate three methods: POPQORN (Ko et al., 2019), our first method based on sampling and linear programming from Section 3.1, denoted as R2 (LP), and our second method based on optimization of the bounds from Section 3.2, denoted as R2 (OPT). Note that OPT also uses LP as its subroutine, as explained in Section 3.2.

As POPQORN is slow, we evaluate this experiment only on 10 correctly classified images randomly sampled from the test set. For each frame index i and each method, we compute the maximum ϵ such that the method can certify that LSTM is robust to perturbations up to ϵ in the L_∞ -norm of the i -th slice of the image. For each method, we compute this maximum ϵ that can be certified using the same binary search procedure as in Ko et al. (2019).

We show the results of this experiment in Fig. 5. First, we observe that perturbations in early frames allow us to certify much smaller ϵ than that in later frames. This is because the approximation error on frame 1 propagates through the later frames to the classifying layer while the error on frame 7 only affects the last layer. Across all frames, both our methods, LP and OPT, outperform POPQORN. We can also see that OPT which can dynamically adjust the bounds can prove more than LP, which uses fixed single linear relaxation per neuron.

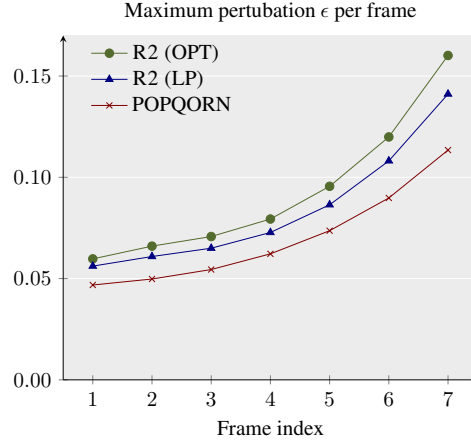
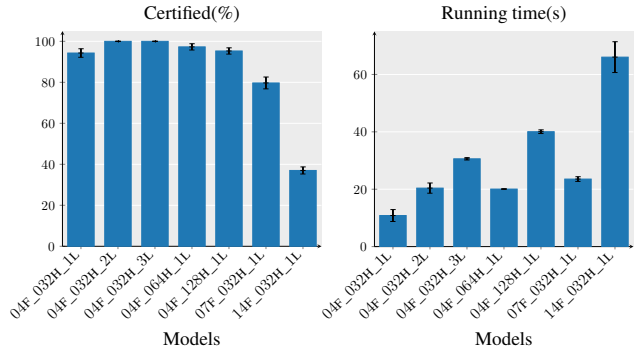


Figure 5. Results for the comparison between R2 and POPQORN. Plotted points represent the maximum L_∞ norm perturbation for each frame index 1 through 7.



(a) Precision over various models

(b) Runtime for a single test over models

Figure 6. Certification of several LSTM models using R2. $F_F_H_H_L_L$ in the label stands for a model consisting of F frames, H hidden units in an LSTM cell, and L layers in the LSTM.

We next compare runtimes of the three methods on perturbations in the first frame – most challenging as it requires propagating through all timesteps. Here, R2 (LP) takes 37 seconds, R2 (OPT) takes 275 seconds and POPQORN takes 2156 seconds per example. Based on this, we conclude that both variants of R2 are more precise than POPQORN while being 50 \times (for LP) and 8 \times more scalable (for OPT).

Scalability demonstration with MNIST In this experiment, we evaluate the scalability of R2 by certifying several recurrent architectures, with varying number of frames, hidden units and LSTM layers. All models have accuracy in the range $96.46 \pm 0.49\%$. For each network, we certify first 100 correctly classified images using the same perturbation $\epsilon = 0.01$ for all frames, with 3 repetitions. While in

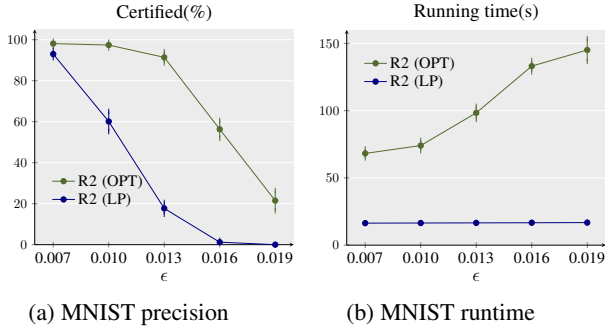


Figure 7. Performance plots of MNIST dataset. All tests are done with 07F_032H_2L.

the previous experiment we certified each frame separately to closely follow the setup from (Ko et al., 2019), it is more natural to assume the adversary is able to perturb the entire input.

We show our results in Fig. 6. Here we first observed the precision of R2 is affected mostly by the number of frames as the precision loss accumulates along the frames. Naturally, running time increases with the number of neurons and frames, as R2 is optimizing the bounds for each $\sigma(x) \tanh(y)$ operation.

However, we also observed a counter-intuitive phenomenon that R2 (OPT) performs better with multiple-layers models than the single-layer model. We performed another experiment with R2 (LP) and found the precision just slightly drops except for 04F_032H_2L and 04F_032H_3L as R2 (LP) results in around 80% precision for both models. Our hypothesis is that an increased number of trainable parameters enhances the flexibility of the bounds for the optimization, allowing us to find more combinations of the bounds which allow certification of the input.

We also tried to plug-in the POPQORN bounds, but it results in precision of 83% and takes an average of 1150 sec per input, even for our smallest model, 04F_032H_1L. As shown in Fig. 6, R2 proves 94.3% for the same model in 10.83 seconds.

Performance demonstration with image classification

In the next experiment, we certify robustness of the MNIST classifier for different ϵ values. We evaluated on 100 correctly classified samples from the test set, performing 10 repetitions. We show our results in Fig. 7. R2 significantly improves the precision: for example for $\epsilon = 0.013$ in Fig. 7a, LP proves 17.7% while OPT certifies 91.4% of samples. These results confirm that learning the bounds dynamically has a large impact on certification precision. In terms of runtime shown in Fig. 7b, OPT naturally consumes more time than LP, but this is justified by the significant in-

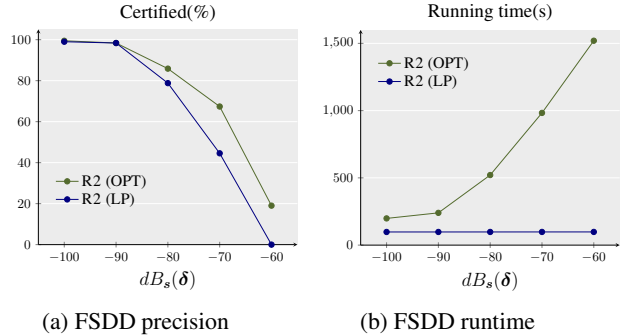


Figure 8. Performance plots of FSDD dataset. All tests are done with the same architecture described in the text.

crease in precision.

5.2. Speech classification

In the next experiment, we certify robustness of a speech classifier on the FSDD dataset (Jackson, 2019). FSDD consists of recordings of digits spoken by 4 different speakers, recorded at 8kHz. Unlike the MNIST task, these tasks are more challenging for LSTM certification as the speech signal is naturally a time series data with variable length. Here we evaluated on the full test set consisting of 200 samples for FSDD, and thus there was no need for repetitions. As POPQORN does not handle speech preprocessing and is too slow for handling long speech signals, we evaluated only our methods.

Preprocessing As mentioned before, one of the key challenges in speech classification, not encountered in the vision domain, is the presence of a complex preprocessing stage before the input is passed to the LSTM network. The preprocessing stage in this experiment consists of FFT and Mel-filter transformations. Preprocessed input is then passed through the fully connected layer with ReLU activation, and then through the LSTM unit. We used the following parameters for the preprocessing: we slice the raw wav signal with length 256 using a step size 200 with 10 Mel-frequencies.

Certifying speech classifier For this experiment, we trained an LSTM network with two LSTM layers and 32 hidden units, preceded by a 40 ReLU-activated fully-connected layer. This network achieves accuracy of 92% on the FSDD task. The average number of frames was 14.7, which is double compared to the previous task on the MNIST dataset.

We use the same decibel (dB) perturbation metric as (Carlini & Wagner, 2018). Given a speech signal s , a decibel of perturbation δ is defined as:

$$dB(s) = \max_i 20 \cdot \log_{10} |s_i|; \quad dB_s(\delta) = dB(\delta) - dB(s).$$

We show the results in Fig. 8. We vary the decibel perturbation between -100 dB and -60 dB and evaluate precision and runtime of R2. Fig. 8a shows percentage of certified samples: our method based on optimizing the bounds (OPT) performs best, e.g., certifying 20% more samples than LP for a significant perturbation of -60 dB. In terms of runtime, Fig. 8b shows that the OPT runtime increases with the perturbation magnitude, meaning that the optimizer needs more iterations to converge to the resulting bounds.

6. Conclusion

We presented a novel approach for certifying recurrent neural networks based on a combination of linear programming and optimization. The key idea was to compute a convex relaxation of the non-linear operations found in the recurrent cells and to be able to dynamically adjust this relaxation according to each input example being certified.

Our experimental results indicate that R2 is both more precise and more scalable than prior work, while offering guarantees on convergence. Thanks to these advances, using R2, we were able to certify, for the first time, the robustness of LSTMs used in speech recognition.

References

- Akintunde, M. E., Kevochian, A., Lomuscio, A., and Pirovano, E. Verification of rnn-based neural agent-environment systems. In *Proceedings of the AAAI Conference on Artificial Intelligence*, 2019.
- Balunovic, M. and Vechev, M. Adversarial training and provable defenses: Bridging the gap. In *International Conference on Learning Representations*, 2020.
- Balunovic, M., Baader, M., Singh, G., Gehr, T., and Vechev, M. Certifying geometric robustness of neural networks. In *Advances in Neural Information Processing Systems*, 2019.
- Biggio, B., Corona, I., Maiorca, D., Nelson, B., Šrndić, N., Laskov, P., Giacinto, G., and Roli, F. Evasion attacks against machine learning at test time. In *Joint European conference on machine learning and knowledge discovery in databases*, 2013.
- Carlini, N. and Wagner, D. Audio adversarial examples: Targeted attacks on speech-to-text. In *2018 IEEE Security and Privacy Workshops (SPW)*, 2018.
- Carlini, N., Mishra, P., Vaidya, T., Zhang, Y., Sherr, M., Shields, C., Wagner, D., and Zhou, W. Hidden voice commands. In *25th {USENIX} Security Symposium ({USENIX} Security 16)*, pp. 513–530, 2016.
- Esmaeilpour, M., Cardinal, P., and Koerich, A. L. A robust approach for securing audio classification against adversarial attacks. *arXiv preprint arXiv:1904.10990*, 2019.
- Gehr, T., Mirman, M., Drachler-Cohen, D., Tsankov, P., Chaudhuri, S., and Vechev, M. Ai2: Safety and robustness certification of neural networks with abstract interpretation. In *2018 IEEE Symposium on Security and Privacy (SP)*, pp. 3–18. IEEE, 2018.
- Gowal, S., Dvijotham, K., Stanforth, R., Bunel, R., Qin, C., Uesato, J., Mann, T., and Kohli, P. On the effectiveness of interval bound propagation for training verifiably robust models. *arXiv preprint arXiv:1810.12715*, 2018.
- Hannun, A., Case, C., Casper, J., Catanzaro, B., Diamos, G., Elsen, E., Prenger, R., Satheesh, S., Sengupta, S., Coates, A., et al. Deep speech: Scaling up end-to-end speech recognition. *arXiv preprint arXiv:1412.5567*, 2014.
- Jackson, Z. Free spoken digit dataset. <https://github.com/Jakobovski/free-spoken-digit-dataset>, 2019.
- Jacoby, Y., Barrett, C., and Katz, G. Verifying recurrent neural networks using invariant inference. *arXiv preprint arXiv:2004.02462*, 2020.
- Katz, G., Barrett, C., Dill, D. L., Julian, K., and Kochenderfer, M. J. Reluplex: An efficient smt solver for verifying deep neural networks. In *International Conference on Computer Aided Verification*, pp. 97–117. Springer, 2017.
- Kingma, D. P. and Ba, J. Adam: A method for stochastic optimization. *arXiv preprint arXiv:1412.6980*, 2014.
- Ko, C., Lyu, Z., Weng, T., Daniel, L., Wong, N., and Lin, D. Popqorn: Certifying robustness of recurrent neural networks. In *International Conference on Machine Learning (ICML)*, 2019.
- LeCun, Y., Cortes, C., and Burges, C. Mnist handwritten digit database. *AT&T Labs [Online]*. Available: <http://yann.lecun.com/exdb/mnist>, 2010.
- Li, J., Qu, S., Li, X., Szurley, J., Kolter, J. Z., and Metze, F. Adversarial music: Real world audio adversary against wake-word detection system. In *Advances in Neural Information Processing Systems*, pp. 11908–11918, 2019.
- Lyu, Z., Ko, C.-Y., Kong, Z., Wong, N., Lin, D., and Daniel, L. Fastened crown: Tightened neural network robustness certificates. *arXiv preprint arXiv:1912.00574*, 2019.
- Mirman, M., Gehr, T., and Vechev, M. Differentiable abstract interpretation for provably robust neural networks.

- In *International Conference on Machine Learning*, pp. 3575–3583, 2018.
- Neekhara, P., Hussain, S., Pandey, P., Dubnov, S., McAuley, J., and Koushanfar, F. Universal adversarial perturbations for speech recognition systems. *arXiv preprint arXiv:1905.03828*, 2019.
- Pachocki, J., Brockman, G., Raiman, J., Zhang, S., Pondé, H., Tang, J., Wolski, F., Dennison, C., Jozefowicz, R., Debiak, P., et al. Openai five. URL <https://blog.openai.com/openai-five>, 2018.
- Papernot, N., McDaniel, P., Swami, A., and Harang, R. Crafting adversarial input sequences for recurrent neural networks. In *MILCOM 2016-2016 IEEE Military Communications Conference*, pp. 49–54. IEEE, 2016.
- Pascual, S., Bonafonte, A., and Serra, J. Segan: Speech enhancement generative adversarial network. *arXiv preprint arXiv:1703.09452*, 2017.
- Paszke, A., Gross, S., Chintala, S., Chanan, G., Yang, E., DeVito, Z., Lin, Z., Desmaison, A., Antiga, L., and Lerer, A. Automatic differentiation in pytorch. 2017.
- Qin, Y., Carlini, N., Goodfellow, I., Cottrell, G., and Raffel, C. Imperceptible, robust, and targeted adversarial examples for automatic speech recognition. In *International Conference on Machine Learning (ICML)*, 2019.
- Raghunathan, A., Steinhardt, J., and Liang, P. Certified defenses against adversarial examples. In *International Conference on Learning Representations*, 2018a.
- Raghunathan, A., Steinhardt, J., and Liang, P. S. Semidefinite relaxations for certifying robustness to adversarial examples. In *Advances in Neural Information Processing Systems, (NeurIPS)*. 2018b.
- Ruan, W., Huang, X., and Kwiatkowska, M. Reachability analysis of deep neural networks with provable guarantees. In *Proc. International Joint Conference on Artificial Intelligence, IJCAI*, pp. 2651–2659, 2018.
- Sahidullah, M. and Saha, G. Design, analysis and experimental evaluation of block based transformation in mfcc computation for speaker recognition. *Speech Communication*, 54(4):543–565, 2012.
- Sainath, T. N., Weiss, R. J., Senior, A., Wilson, K. W., and Vinyals, O. Learning the speech front-end with raw waveform cldnns. In *Sixteenth Annual Conference of the International Speech Communication Association*, 2015.
- Salman, H., Yang, G., Zhang, H., Hsieh, C., and Zhang, P. A convex relaxation barrier to tight robustness verification of neural networks. In *Advances in Neural Information Processing Systems, (NeurIPS)*, 2019.
- Shi, Z., Zhang, H., Hsieh, C.-J., Chang, K.-W., and Huang, M. Robustness verification for transformers. In *International Conference on Learning Representations*, 2020.
- Singh, G., Gehr, T., Mirman, M., Püschel, M., and Vechev, M. T. Fast and effective robustness certification. In *Advances in Neural Information Processing Systems, (NeurIPS)*, 2018.
- Singh, G., Ganvir, R., Püschel, M., and Vechev, M. Beyond the single neuron convex barrier for neural network certification. In *Advances in Neural Information Processing Systems*, 2019a.
- Singh, G., Gehr, T., Püschel, M., and Vechev, M. An abstract domain for certifying neural networks. *Proceedings of the ACM on Programming Languages*, 3(POPL): 41, 2019b.
- Singh, G., Gehr, T., Püschel, M., and Vechev, M. Boosting robustness certification of neural networks. In *International Conference on Learning Representations*, 2019c.
- Szegedy, C., Zaremba, W., Sutskever, I., Bruna, J., Erhan, D., Goodfellow, I., and Fergus, R. Intriguing properties of neural networks. *arXiv preprint arXiv:1312.6199*, 2013.
- Vinyals, O., Babuschkin, I., Chung, J., Mathieu, M., Jaderberg, M., Czarnecki, W. M., Dudzik, A., Huang, A., Georgiev, P., Powell, R., et al. Alphastar: Mastering the real-time strategy game starcraft ii. *DeepMind blog*, pp. 2, 2019.
- Wang, S., Pei, K., Whitehouse, J., Yang, J., and Jana, S. Efficient formal safety analysis of neural networks. In *Advances in Neural Information Processing Systems, (NeurIPS)*. 2018a.
- Wang, S., Pei, K., Whitehouse, J., Yang, J., and Jana, S. Formal security analysis of neural networks using symbolic intervals. In *27th {USENIX} Security Symposium ({USENIX} Security 18)*, pp. 1599–1614, 2018b.
- Weng, T., Zhang, H., Chen, H., Song, Z., Hsieh, C., Daniel, L., Boning, D. S., and Dhillon, I. S. Towards fast computation of certified robustness for relu networks. In *International Conference on Machine Learning, (ICML)*, 2018.
- Wong, E. and Kolter, J. Z. Provable defenses against adversarial examples via the convex outer adversarial polytope. *arXiv preprint arXiv:1711.00851*, 2017.
- Wu, M. and Kwiatkowska, M. Robustness guarantees for deep neural networks on videos. *arXiv preprint arXiv:1907.00098*, 2019.

Yang, Z., Li, B., Chen, P.-Y., and Song, D. Characterizing audio adversarial examples using temporal dependency. 2019.

Zhang, H., Weng, T., Chen, P., Hsieh, C., and Daniel, L. Efficient neural network robustness certification with general activation functions. In *Advances in Neural Information Processing Systems, (NeurIPS)*, 2018.

Zhang, H., Chen, H., Xiao, C., Goyal, S., Stanforth, R., Li, B., Boning, D., and Hsieh, C.-J. Towards stable and efficient training of verifiably robust neural networks. In *International Conference on Learning Representations*, 2020.

A. Details on Offset Adjustment

A.1. Boundings for $\sigma(x) \tanh(y)$

Here we provide details of Step 2 from Section 3.1. Let $x \in [l_x, u_x]$, $y \in [l_y, u_y]$, and $A_l x + B_l y + C_l$ be the initial lower bounding plane obtained from LP. We define $F(x, y)$ as:

$$F(x, y) = \sigma(x) \tanh(y) - (A_l x + B_l y + C_l)$$

To find $\Delta_l = \max_{x,y} F(x, y)$, we first find the extreme points by computing partial derivatives.

$$\frac{\partial F}{\partial x} = \sigma(x) \tanh(y) (1 - \sigma(x)) - A_l \quad (3)$$

$$\frac{\partial F}{\partial y} = \sigma(x) \tanh(y) (1 - \tanh^2(y)) - B_l \quad (4)$$

Case 1: $x \in \{l_x, u_x\}$ Under this condition, we denote $S_x := \sigma(x)$ as a constant. To ease the notation, let $t = \tanh(y)$ where $t \in [\tanh(l_y), \tanh(u_y)]$. Then $\frac{\partial F}{\partial y} \stackrel{!}{=} 0$ can be rewritten as

$$t(1 - t^2) = \frac{B_l}{S_x} \quad (5)$$

Case 2: $y \in \{l_y, u_y\}$ Here we set $T_y := \tanh(y)$ and $s = \sigma(x)$, $x \in [\sigma(l_x), \sigma(u_x)]$ analogously. $\frac{\partial F}{\partial x} \stackrel{!}{=} 0$ can be rewritten as

$$s(1 - s) = \frac{A_l}{T_y} \quad (6)$$

Case 3: otherwise Otherwise, we consider both $\frac{\partial F}{\partial x} \stackrel{!}{=} 0$ and $\frac{\partial F}{\partial y} \stackrel{!}{=} 0$. By combining Eq. (3) and Eq. (4), we reduce $\tanh(y)$ and obtain

$$s^4 + (-2 - B_l)s^3 + (1 + 2B_l)s^2 + (-B_l)s - A_l^2 \stackrel{!}{=} 0 \quad (7)$$

The proper roots of above expressions make up the candidates for the extreme points of F . Hence, it is sufficient to compare the value of F at the roots of Eq. (5), Eq. (6), and Eq. (7), and the 4 corner coordinates to get Δ_l in the given domain. By replacing $C_l \leftarrow C_l - \Delta_l$, modified F is no greater than 0, which means the plane is always equal or strictly below the $\sigma(x) \tanh(y)$ curve.

We can follow the analogous process for the upper bound of the curve.

A.2. Boundings for $\sigma(x)y$

We briefly note that another operation, $\sigma(x)y$, appearing in LSTM cell, is generally similar to the case of $\sigma(x) \tanh(y)$,

but there is no need to calculate inner-border extreme points. Let $G(x, y) = \sigma(x)y - (A_l x + B_l y + C_l)$.

$$\frac{\partial G}{\partial x} = \sigma(x)y(1 - \sigma(x)) - A_l \quad (8)$$

$$\frac{\partial G}{\partial y} = \sigma(x) - B_l \quad (9)$$

Case 1: $x \in \{l_x, u_x\}$ When $\sigma(x)$ is fixed, Eq. (9) is constant, which means G is monotonous in this case.

Case 2: $y \in \{l_y, u_y\}$ Denote $s = \sigma(x)$ where $s \in [\sigma(l_x), \sigma(u_x)]$, then setting Eq. (8) $\stackrel{!}{=} 0$ becomes

$$s(1 - s) = \frac{A_l}{y} \quad (10)$$

Case 3: otherwise If there is a local extremum in the region, Hessian of G must be either positive-definite or negative-definite.

$$\frac{\partial^2 G}{\partial x^2} = \sigma(x)y(1 - \sigma(x))(1 - 2\sigma(x))$$

$$\frac{\partial^2 G}{\partial y^2} = 0$$

$$\frac{\partial^2 G}{\partial x \partial y} = \sigma(x)(1 - \sigma(x))$$

$$\frac{\partial^2 G}{\partial x^2} \cdot \frac{\partial^2 G}{\partial y^2} - \left(\frac{\partial^2 G}{\partial x \partial y} \right)^2 = -(\sigma(x)(1 - \sigma(x)))^2 < 0$$

Hence, there is no local maximum inside the boundaries.

Wrapping up, we only need to consider the roots of the Eq. (10) and the 4 corners to calculate the maximum of G to get Δ_l for $\sigma(x)y$. Upper bound is analogous to this calculations.

By above mentioned offset adjustment by Δ_l or Δ_u (for upper bounding plane), Our proposed planes are guaranteed to ensure soundness.

B. Asymptotic Optimality of LP boundings

To provide guarantees on our bounds, we apply the following theorem from Balunovic et al. (2019):

Theorem 1. *Let N be the number of points sampled in our algorithm and ϵ the tolerance used in the Lipschitz optimization. Let (ω_l, b_l) be our lower constraint and let (ω^*, b^*) be the minimum of L . For every $\delta > 0$ there exists N_δ such that $|L(\omega_l, b_l) - L(\omega^*, b^*)| < \delta + \epsilon$ for every $N > N_\delta$, with high probability. Analogous result holds for upper constraint (ω_u, b_u) and function U .*

where, roughly saying, $L = \int_{(x,y)} F(x,y)$ and analogous for the upper bound case U , and (ω_l, b_l) are our A_l, B_l, C_l . As we do not perform the Lipschitz optimization, but instead compute the closed-form solution, our approximation corresponds to the case $\epsilon = 0$ here, and the theorem guarantees the asymptotic optimality of our bounds.